Retinoic Acid Receptor Gamma Activity Plays a Critical Role in Regulating Early Mouse Gastruloid Development

Jide T. Olanipekun , Benjamin Edginton-White , Caitlin McQueen , Geoffrey Brown * , William E.B. Johnson *

Posted Date: 1 April 2026

doi: 10.20944/preprints202603.2526.v1

Keywords: all *trans* retinoic acid; retinoic acid receptorγ; embryonic development; gastruloid; axial patterning; cell fate; cell differentiation

 doi:10.20944/preprints202603.2526.v1

Article

Retinoic acid Receptor γ Activity Plays a Critical Role in Regulating Early Mouse Gastruloid Development

Jide T. Olanipekun [1], Benjamin Edginton-White [2], Caitlin McQueen [3], Geoffrey Brown [3,*] and William E.B. Johnson [1,*]

[1] Chester Medical School, University of Chester, Chester CH1 4BJ, UK
[2] Department of Cancer and Genomic Sciences, School of Medical Sciences, College of Medicine and Health, University of Birmingham, Birmingham, B15 2TT, UK
[3] Biological Sciences, University of Chester, Chester CH1 4BJ, UK
[4] Department of Biomedical Sciences, School of Infection, Inflammation, and Immunology, College of Medicine and Health, University of Birmingham, Birmingham, B15 2TT, UK
* Correspondence: g.brown@bham.ac.uk; eustace.johnson@chester.ac.uk

Abstract

Regulation of all-*trans* retinoic acid (ATRA) signalling is crucial to early embryonic development. We show here that in embryonic stem (ES) cell-derived gastruloids, which mimic normal development in response to the Wnt/β-catenin agonist CHIR9901, expression of retinoic acid receptor (RAR)γ was spatially restricted to primitive cells that co-expressed ES cell and early progenitor cell markers, i.e., Nanog, Sox2, and Oct4. In contrast, RARα expression was ubiquitous. mRNAs for the key enzymes involved in ATRA synthesis (Aldh1a2) and degradation (Cyp26a1) were not seen in cells that expressed RARγ. Treatment of ES cell-derived gastruloids with physiologically relevant (10nM) levels of ATRA or with a highly selective RARγ agonist blocked normal developmental processes, preventing symmetry-breaking and axial elongation. This was not seen following treatments with an RARα agonist, where there was a tendency for enhanced axial elongation. Brachyury (TBXT) immuno-positive cells localised in the posterior end of elongated gastruloids in control- and RARα agonist-treated cultures, with Sox2 immuno-positive cells seen more widely, whilst both TBXT and Sox2 immuno-positive cells were randomly distributed throughout ATRA- and RARγ agonist-treated gastruloids. Concurrent treatment of gastruloids with 10nM ATRA and 100nM of an RARγ antagonist partially abrogated the ATRA-mediated block to axial elongation. Conversely, 10nM RARγ antagonist treatments were associated with the formation of multi-axis gastruloid elongations, with comparatively little effect seen after treatments with an RARα antagonist. These findings reveal that RARγ plays a crucial role in the development of embryonic tissues.

Keywords: all *trans* retinoic acid; retinoic acid receptorγ; embryonic development; gastruloid; axial patterning; cell fate; cell differentiation

1. Introduction

A small and defined set of signalling pathways are used by the embryo during early development, which, when integrated over time, orchestrate axial patterning and morphogenesis to unfold the body plan. All-*trans* retinoic acid (ATRA), the major active metabolite of vitamin A, is a key signalling molecule. It inputs to many stages of development to regulate stem cell fate, axial development [1] and the generation of differentiated tissues, e.g. neuronal, cardiac, pancreatic, lung, and the eye [2-3]. ATRA activity is undetectable in the mouse embryo prior to embryonic day (E) 7.5 (approximately); however, following the formation of the mesoderm, ATRA activity occurs along the primitive streak, throughout the posterior portion of the embryo and within the nascent mesoderm [4]. At later developmental stages, its activity is reduced in the tailbud, present in all tissues of the

 doi:10.20944/preprints202603.2526.v1

embryo trunk up to the boundary between the hindbrain and the first somite, and within optic lobes and the surrounding mesenchyme in the prospective head region [4, reviewed in 5].

A correct balance to the spatial and temporal distribution of ATRA synthesis and its activity is critical to the proper embryonic development [6-9], as environmental, genetic, or experimental perturbations that target ATRA signalling (either positively or negatively) cause wide-ranging abnormalities [6,10]. Accordingly, tissue access to ATRA within the developing embryo is tightly regulated through the activity of enzymes that control its synthesis from vitamin A, i.e., through retinol dehydrogenase (Rdh10) and aldehyde dehydrogenase (Ald1A2) activity and its catabolism, through cytochrome P450 (Cyp26a1) activity [5]. Prior to gastrulation, Cyp26a1 is expressed throughout the embryo as a protective barrier against maternal ATRA [11]. By E7.25, Cyp26a1 expression occurs in the primitive streak following its progression anteriorly by E7.5 [12], and by E9.0 is confined to the tailbud [13]. Aldh1a2 on the other hand, the key enzyme in the final formation of ATRA, is first detected in the primitive streak and nascent mesoderm of E7.5 embryos, co-localises with ATRA signalling, and forms a distinct signalling boundary with the expression of Cyp26a1 [14]. The ATRA concentration gradients that are established by the reciprocal actions of Rdh10, Ald1A1 and Cyp25A1 are constantly modified throughout embryo development, and the changing gradients regulate signalling from other pathways that orchestrate morphogenesis also in a spaciotemporal manner as provided, for example, by Wnts, transforming growth factors (TGFs) and fibroblast growth factors (FGFs) [15-16].

ATRA is the ligand for the three main isoforms of the retinoic acid receptors (RARs; RAR α, RAR β and RAR γ). They bind to the *cis*-acting response elements of ATRA target genes as a heterodimer with retinoid X receptor and changes to transcription of downstream developmental genes occurs following the engagement of ATRA with RARs [17]. The gene expression pathways that are ATRA-regulated via RARs are essential for normal embryonic development and cellular differentiation [10,18,19]. Embryonic stem (ES) cells, derived from the inner cell mass of the preimplantation blastocyst, have the capacity to differentiate into all cell and tissue types of the embryo. Therefore, they are an attractive model to study stem and progenitor cell-fate decisions and differentiation during early embryonic development [20]. When 200-300 ES cells are aggregated in 3D suspension cultures they form spheroids and when pulsed with the Wnt/β-catenin agonist CHIR99021 (CHIR) between 48-72 hours, they recapitulate many aspects of early development [21,22]. After around 120 hours of culture, the ES cells form so-called ‘gastruloids’, wherein 3D ES spheroids progressively break symmetry, polarise gene expression, can form 3 orthogonal axis (anteroposterior, dorsoventral, mediolateral) and undergo axial elongation [21-23]. Pulsing with CHIR is essential for consistently reproducible axial elongation, but this is blocked by treating mouse and human gastruloid cultures with 0.4 nM-33 nM concentrations of ATRA [24]. However, there is some confusion regarding the precise influence of ATRA on the fate of treated ES cells. For example, other research reported that generating human gastruloids using a combination of CHIR, the extracellular matrix components in Matrigel, and treating with two different concentrations of ATRA exogenously at different times, i.e., with 500nM ATRA in the earlier stages of ES spheroid formation (0-24 hours) and 100nM ATRA in the later stages of gastruloid elongation (48-120 hours) resulted in the robust formation of elongated gastruloids with neural tubes and somite-like structures [25].

The roles of physiological levels of ATRA (approximately 5nM-20nM) [26-28] in determining ES cell fate during embryonic development and particularly in roles of individual RAR isoforms remain unclear. The concentrations of ATRA used in many studies are generally not within the physiological range. For example, whilst pharmacological concentrations of ATRA (0.5μM-5mM) have been used routinely to induce neuronal differentiation [25,29], 1.6μM ATRA was shown to increase the presence of more primitive 2 cell-like totipotent cells (2CLCs) in ES cell cultures, which was largely due to activation of RARγ [30], and a lower level of ATRA levels (100 nM) induced the expression of mesodermal marker genes within mouse ES cells [31]. As gastruloids provide a highly tractable *in vitro* model for developmental studies, here we have examined the expression of RAR isoforms within the cell compartments in gastruloids to determine their potential association with

 doi:10.20944/preprints202603.2526.v1

developmental processes. Previously, we developed synthetic retinoids that were shown in transactivation studies to be highly specific for each of the RARs in the nanomolar range [32]. Therefore, we have combined information provided bioinformatic analyses that examined the presence of RARs in developing gastruloids with findings for the influence of 10nM treatments of ATRA and of highly specific RAR agonists and antagonists on gastruloid development. This enabled us to examine how signals provided by the activities of RARα and RARγ, as governed by the spatial availability of ATRA, and Wnt/β-catenin signalling, are integrated to control tissue patterning and tissue formation. We show that RARγ activity plays a critical role in determining the progression of early embryonic development.

2. Results

2.1. The Expression of RARα and RARγ During Gastruloid Development

Levels of mRNA for RARα and RARγ, as identified using single cell RNA sequencing in days 4-7 of gastruloid development [33](downloaded from the Gene Expression Omnibus, accession number: GSE158999) were correlated with the expression of genes that are associated with different cell and developing tissue types. These data are shown as violin plots in **Figure 1**. As shown, RARα expression was largely present across all cell and tissue types (**Figure 1A**). In contrast, RARγ expression was more restricted across developing tissues and was highly expressed only in those primitive tissues that contained prominent stem/progenitor cell compartments, i.e., the epiblast, NMPs, caudal epiblasts, caudal mesoderm, rostral neuroectoderm, and the primitive streak (**Figure 1B**).

 doi:10.20944/preprints202603.2526.v1

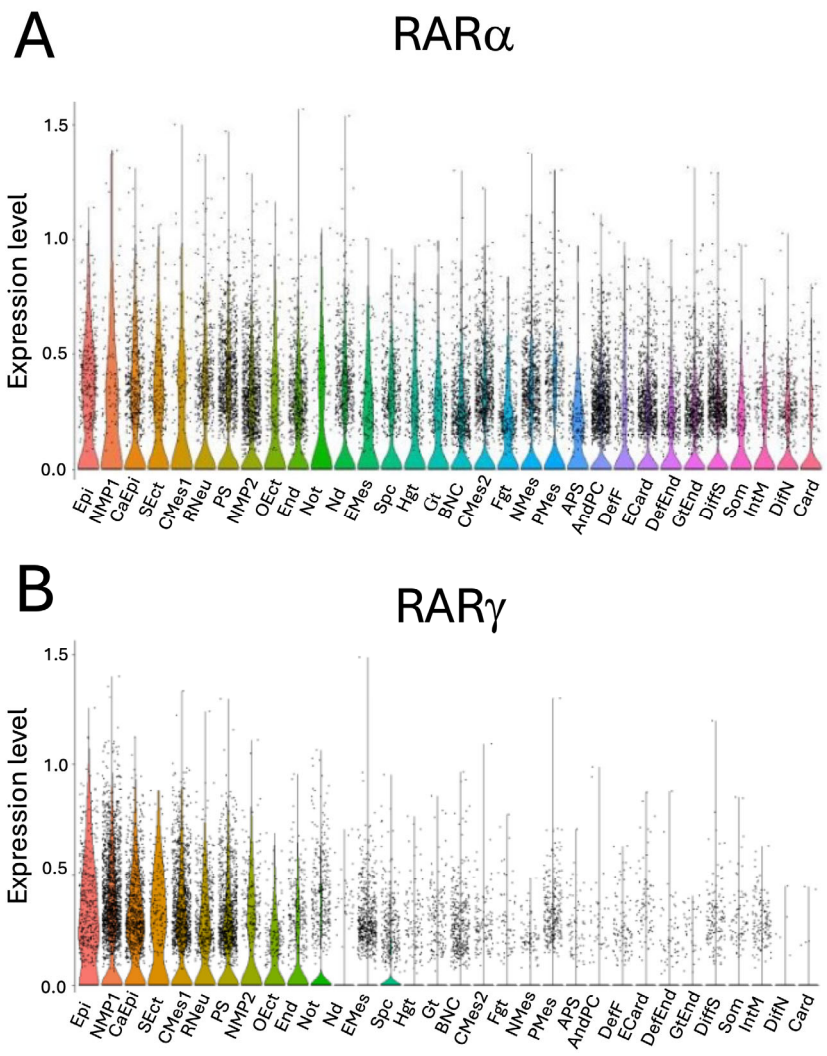

Figure 1. Expression of RARα and RARγ within mouse ES cells in gastruloid culture. Single cell mRNA-seq datasets for gastruloids across four time points (days 4-7) were obtained from [33]. Using the previously identified cell type clusters [33], violin plots were produced to identify cell type specific gene expression. (A) RARα mRNA was present in all the identified cell and tissue types. (B). RARγ mRNA was restricted to fewer cell and tissue types, and was strongly expressed in the NMPs, caudal epiblast, caudal mesoderm, rostral neuroectoderm, and primitive streak.

Abbreviations: Epi: epiblast; NMP1 : neuromesodermal progenitor; CaEpi: caudal epiblast; SEct: surface ectoderm; CMes1: caudal mesoderm; RNeu: rostral neuroectoderm; PS: primitive streak; NMP2: neuro mesodermal progenitors (mesoderm); OEct: oral ectoderm; End: endothelium; Noto: notochord; Nd: node; EMes: early mesoderm; Spc: Spinal cord; Hgt: hindgut; Gt: gut; BNC: brain, neural crest; CMes2: cardiac mesoderm; Fgt: foregut; NMes: nascent mesoderm; PMes: pharyngeal mesoderm; APS: anterior primitive streak; ANDPC: hematoendothelial progenitors: DefF: definitive front; Ecard: early cardiomyocytes; DefEnd: definitive endoderm; GtEnd: gut/visceral endoderm; DiffS: differentiated somite: Som: somite/sclerotome; IntM: intermediate mesoderm; DifN: differentiated neurons: Card: cardiomyocytes.

Next, we explored the phenotype of cells that expressed RARα and RARγ both in relation to each other and the expression of the ATRA metabolizing enzymes, Cyp26a1 and Aldh1a2 and also in relation to pluripotent stem cell and development regulatory-associated transcription factors, i.e., Nanog, Oct4, Sox2, Sox1, and brachyury (TBXT). A heatmap showing the Pearson correlation for co-

 doi:10.20944/preprints202603.2526.v1

expression of these various gene pairs across all cells in gastruloids during days 4-7 is shown in **Figure 2**. RARα and RARγ were not expressed in the same cells. There were no marked correlations between RARα expression with the expression levels for the pluripotent stem cell genes, i.e., Nanog or Oct4, nor with TBXT. In contrast, there were strong positive correlations between RARγ expression with Nanog, Oct4, as well as Sox2 and TBXT. RARγ expression did not correlate with Cyp26a1, Aldh1a2 and Sox 1 expression. This analysis shows that the cells in gastruloids that express RARγ are primitive in nature and that they are dependent on exogenous ATRA levels for ATRA regulated processes.

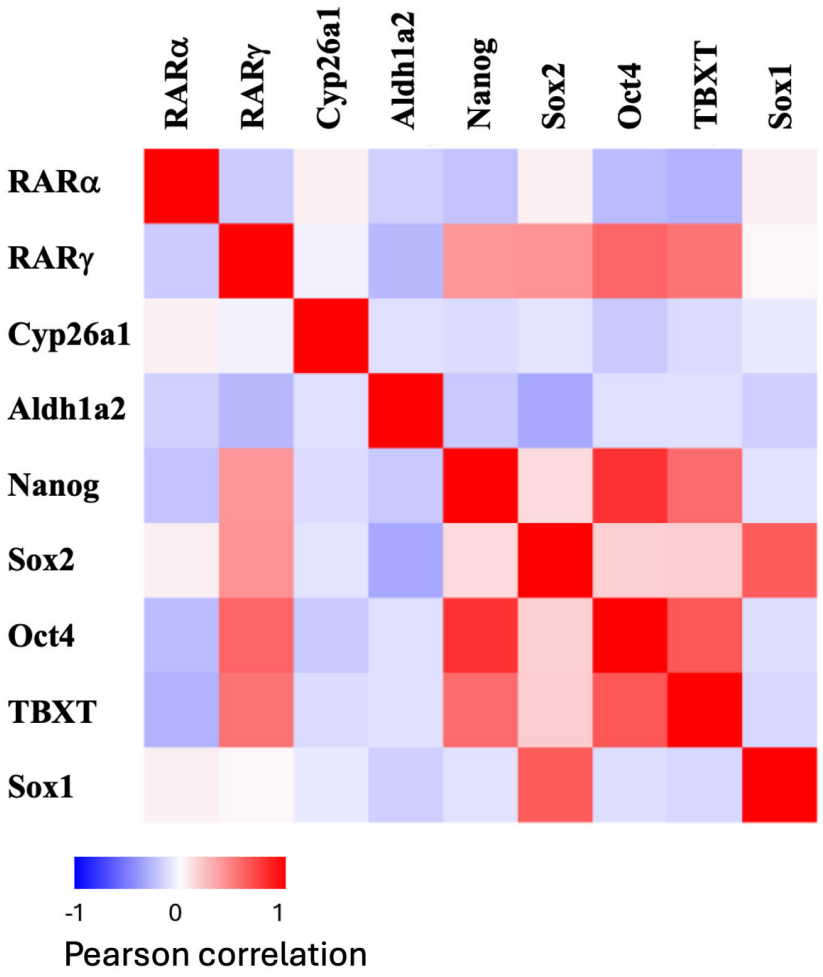

Figure 2. RARγ expression correlates with gene expression of stem cell/developmental transcription factors. The heatmap shows the Pearson rank correlation of gene pairs across all cell types and combined days based on the expression of genes in metacells. There is a positive correlation between RARγ mRNA levels with that of Nanog, Sox2, Oct4, and TBXT mRNAs. In contrast, there was no marked correlation of RARα mRNA expression with these genes in all cells. For the enzymes involved in ATRA synthesis (Aldh1a2) and degradation (Cyp26a1), the cells that expressed RARγ mRNA did not express mRNAs for these enzymes. .

2.2. The Effects of ATRA and RARa and RARγ Specific Agonists and Antagonists on Gastruloid Development

Having observed that RARs were differentially expressed in developing gastruloids, and that the cells that expressed RARγ do not express the enzymes required for ATRA synthesis or degradation, we examined the effects of treating gastruloids with physiological levels of exogenous ATRA and RAR isoform-specific synthetic retinoids. When aggregates of ES cells were stimulated

 doi:10.20944/preprints202603.2526.v1

with the Wnt/β catenin agonist CHIR from 48-72 hours of culture in N2B27 media, which is the standard culture condition for the generation of gastruloids, they broke symmetry and underwent axial elongation by 120 hours. This also was seen for DMSO treated cultures, i.e., carrier controls in N2B27 media. However, when 10nM ATRA was also added to CHIR-stimulated ES aggregates at 48-72 hours, there was a complete block in symmetry breaking and no axial elongation at 120 hours. Treatments with 10nM of the RARγ agonist AGN205327 over the same period had the same effect, i.e., there was a complete block in symmetry breaking and no axial elongation. All of the ATRA- and RARγ agonist-treated cultures were spheroidal at 120 hours. Conversely, treatments of CHIR-stimulated ES aggregates with 10nM of the RARα agonist AGN195183 from 48-72 hours led to symmetry breakage and the gastruloids had undergone axial elongation by 120 hours.

ES aggregates treated with either 10nM ATRA or 10nM RARγ agonist had marked and significant reductions in their measured elongation indices (indicating gastruloid shape) and overall lengths at 120 hours compared with the gastruloids in standard inductions in N2B27 medium and in the DMSO carrier control cultures. There was a moderate increase in the elongation index and length of 10nM RARα agonist-treated gastruloids at the same time point, which was significantly greater than the N2B27 control cultures, but not the DMSO control cultures. Most of CHIR-stimulated ES aggregates treated with 10nM of the RARα antagonist AGN196996 or of the RARγ antagonist AGN205728 from 48-72 hours broke symmetry and underwent axial elongation by 120 hours. It was noteworthy also that there was a tendency for some gastruloids in all conditions that included DMSO, i.e., all except the N2B27 control cultures, to form multiaxis elongations, and that this phenotype was most prevalent in the 10nM RARγ antagonist-treated cultures (**Figure 3**).

 doi:10.20944/preprints202603.2526.v1

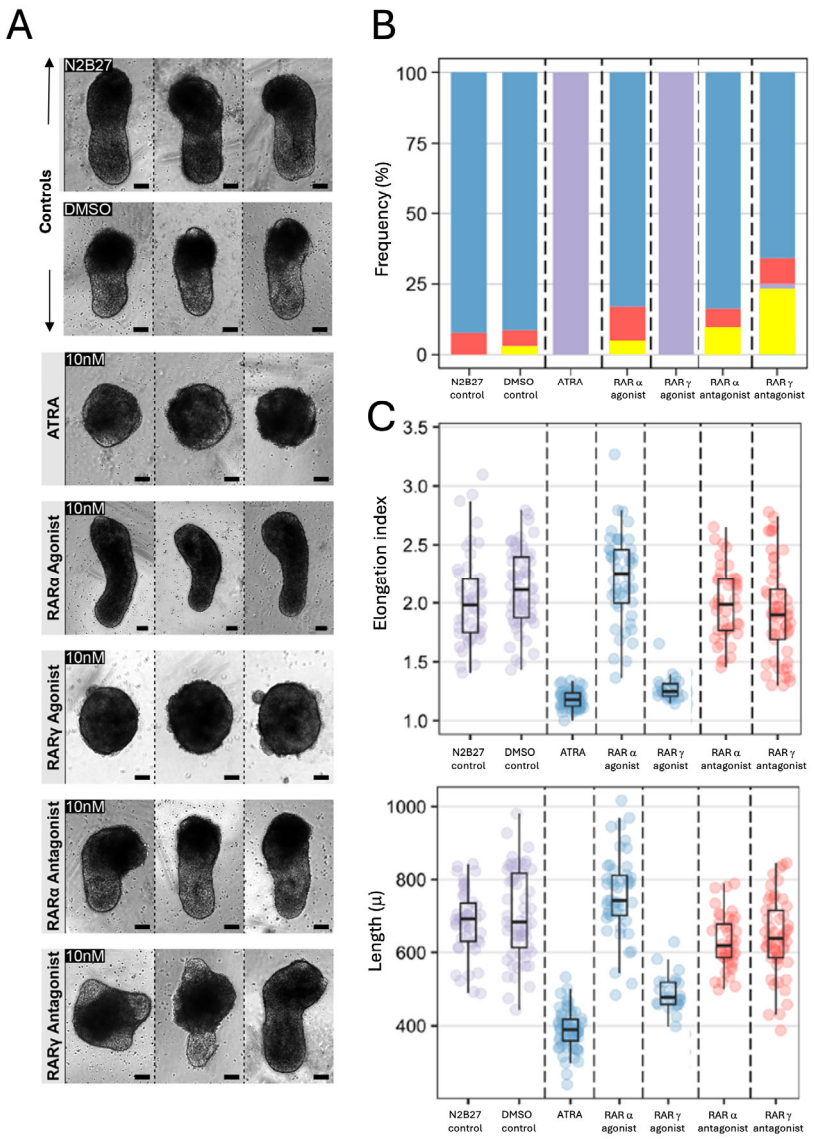

Figure 3. Physiological levels of 10nM ATRA and 10nM RARγ agonism blocked gastruloid axial elongation. **(**A). Representative brightfield images from at least three independent samples (biological repeats) are shown for gastruloids at 120 hours that had been cultured in N2B27 medium for 48 hours and stimulated with a pulse of 3 μM CHIR between 48-72 hours along with gastruloids treated identically but with either DMSO or ATRA or specific agonists and antagonists of RARγ or RARα. The medium was replaced with fresh N2B27 without any supplementation at 72 and 96 hours. Gastruloids were imaged and fixed at 120 hours. ATRA and selective RARγ agonism blocked axial elongation, whereas RARα agonism did not. All scale bars are 100μ. (B). The proportions of gastruloids that were classified as elongated (blue), ovoid (red), spheroid (purple) or multiaxis (yellow) in each experimental group at 120 hours of culture. As shown, ATRA and RARγ treatment blocked axial elongation. (C). The elongation indices and lengths of gastruloids in each experimental group at 120 hours of culture. There were significant differences in these measures between the DMSO carrier control group and the ATRA- and RARγ agonist-treated groups ($p<0.001$), and between the RARα agonist-treated group ($p<0.05$) versus the N2B27 control group, but not the DMSO carrier control group. (Kruskal-Wallis). Data are shown as box and whisker plots, with values pooled from n=3 independent experiments.

We next examined the presence of key transcription factors that are known to localize differentially during gastruloid formation. Immunostaining showed that TBXT was present at 120

 doi:10.20944/preprints202603.2526.v1

hours localized to the posterior end of gastruloids in DMSO control cultures and RARα agonist-, RARα antagonist-, and RARγ antagonist-treated cultures, all of which had elongated to a similar extent. Conversely, TBXT immuno-positivity was seen to be localized to clusters of cells throughout the ATRA- and RARγ agonist-treated gastruloid cultures, which were spheroidal at 120 hours after treatment. Hence, it was clear that TBXT immune-positive cells were only localized in those gastruloids that had broken symmetry and undergone axial elongation. Interestingly, we also observed that TBXT was seen in the tips of multiaxis elongations, in many but not all cases. Immunopositivity for Sox2 was seen in all gastruloids, often in the proximity of TBXT cells, but without direct co-localization. In the ATRA- and RARγ agonist-treated cultures, Sox-2 was seen in groups of clustered cells, suggesting compartmentalization, but the distributions of these clusters appeared randomly throughout the spheroids. There were no clear differences in the intensity of TBXT or Sox2 in any of the experimental groups, suggesting a similar level of expression of these transcription factors (**Figure 4**).

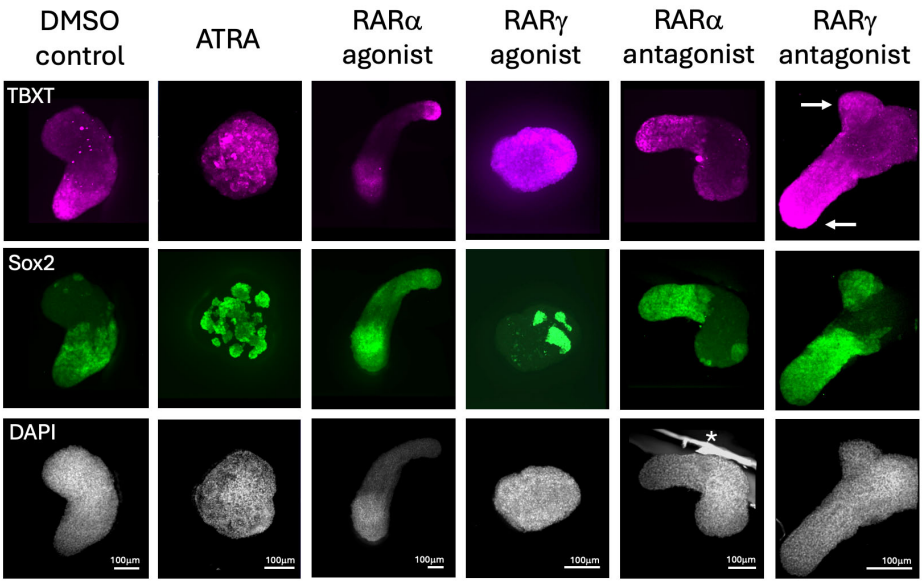

Figure 4. TBXT and Sox2 immunopositivity in gastruloids treated with ATRA and RAR specific agonists and antagonists. Representative fluorescence images are shown after TBXT and Sox2 immunohistochemistry and confocal microscopy using projected images of z stacks of gastruloids at 120 hours that had been stimulated with 3 µM CHIR between 48-72 hours along with either DMSO (carrier control cultures) or with 10nM ATRA or 10nM of agonists and antagonists specific for RARγ or RARα. As shown, TBTX localized in the posterior tips of gastruloids that had successfully elongated with Sox2 immuno-positive cells present in adjacent tissue. In contrast, clusters of TBXT and Sox2 immuno-positive cells were seen randomly distributed in the ATRA- and RARγ agonist treated ES cultures which remained as spheroids. Interestingly, TBXT and adjacent Sox2 immunopositivity were seen in in the tips of outgrowing branches of those gastruloids that underwent multiaxis elongation (arrowed in RARγ antagonist-treated culture). There were n=3 independent experiments (biological repeats). All scale bar are 100µ (*artefact).

2.3. The Inhibitory Effects of ATRA on Gastruloid Axial Elongation Were Partially Abrogated by RARγ Specific Antagonism

Finally, in separate experiments we tested whether the effects of 10nM ATRA-treatment could be abrogated by concurrent treatments with the RARγ antagonist, using an excess concentration of 100nM of the antagonist. Markedly more ovoid morphologies were seen at 120 hours regarding the gastruloids treated with ATRA plus RARγ antagonist as compared with the ATRA alone-treated group, to greater than 50% of all gastruloids. Furthermore, there was a subtle but nonetheless

 doi:10.20944/preprints202603.2526.v1

significant difference in both the elongation index and the overall length of the gastruloids in the ATRA plus RARγ antagonist-treated group compared with the ATRA alone-treated group. Treatments with 100nM RARγ antagonist alone were associated with axial elongation, as seen in control groups (**Figure 5**).

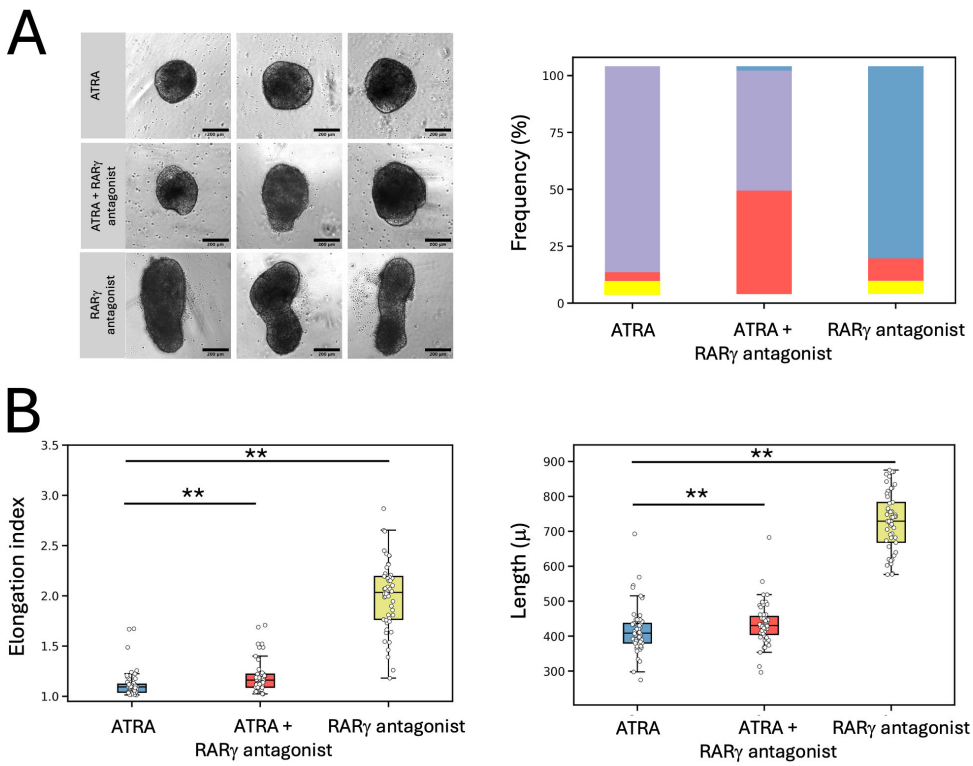

Figure 5. ATRA-mediated block in gastruloid axial elongation was partially abrogated by RARγ antagonism. (A). Left panel: Representative brightfield images are shown of gastruloids at 120 hours that had been stimulated with 3 μM CHIR between 48-72 hours and treated at the same time with 10nM ATRA or with 10nM ATRA plus 100nM of an RARγ antagonist or with 100nM RARγ antagonist. All scale bards are 200μ. Right panel: the frequency of gastruloid cultures under these conditions that were spheroid (purple bars), ovoid (red bars), elongated (blue bars) or multiaxis (yellow bars). As shown, there was a marked increase in the presence of ovoid gastruloids when RARγ antagonism was combined with ATRA. (B). The elongation indices and lengths of gastruloids in each experimental group at 120 hours of culture. There were significant differences in these measures between the ATRA-alone versus the ATRA plus RARγ antagonist-treated group, between the ATRA-alone versus the RARγ antagonist-treated group, and between the ATRA plus RARγ antagonist-treated group versus the RARγ antagonist-treated group (**p<0.01). (Kruskal-Wallis). Data are shown as box and whisker plots, with values pooled from n=3 independent experiments.

3. Discussion

We have explored the roles of specific RARs in the regulation of retinoic acid signaling in early embryonic development using ES-derived gastruloids as a model system and highly specific RAR agonists and antagonists at physiological concentrations. We show that RARγ is expressed specifically in stem/progenitor cell compartments of developing gastruloids, whereas the expression of RARα is widespread. We also show that the enzymes needed for ATRA synthesis, Aldh1a2, and catabolism, Cyp26a1, are not expressed by RARγ positive cells. Further, we have shown that treatments with physiological levels of exogenous ATRA or with an RARγ specific agonist blocked the development of mouse ES-derived gastruloids in response to stimulation of the Wnt/β catenin

 doi:10.20944/preprints202603.2526.v1

signalling pathway. Axial elongation was ablated in these conditions. Conversely, 10nM RARα agonist treatments of gastruloids tended to increase axial elongation. These data show that the effects of ATRA in blocking axial elongation during gastruloid development are mediated through RARγ activity.

Previously, we showed that treating zebrafish embryos at 4 hours post-fertilization with 10nM-80nM of the RARγ specific agonist AGN205327, in the absence of exogenous ATRA, disrupted the formation of many tissues, which was not seen following treatments with the RARα specific agonist AGN195183 [18]. A block to stem/progenitor cell differentiation led to severe truncation of the embryonic zebrafish, with fewer somites in the tail, loss of the most posterior regions of the trunk including the caudal fin, and a lack of pectoral fin, reduced craniofacial bones and anterior neural ganglia. The RARγ agonist also blocked caudal fin regeneration when the fin was transected at 2-3 days post embryo fertilization. RARγ agonism did not lead to a loss of the Tbx-5^{+} lateral plate mesodermal stem/progenitor cells, because these cells were still present after RARγ agonist treatment and the block to pectoral fin development was reversible if the RARγ agonist in the zebrafish water was washed out or if an RARγ antagonist was added to the water. Furthermore, washouts of the RARγ agonist or co-treatments with an RARγ antagonist restored caudal fin regeneration. Here, we found that TBXT and Sox2 immuno-positive cells remained in ATRA- and RARγ agonist-treated ES-derived gastruloids, which, similarly to zebrafish, had been blocked in development. TBXT and Sox2 are key regulators of gastruloid development [34], with TBXT activity in particular determining symmetry breaking and the extent of axial elongation [21,35]. The presence of TBXT and Sox2 immuno-positive cells in the ATRA and RARγ agonist treated cultures suggested that these gastruloids maintained a capacity for development. Furthermore, we found that adding an excess level of RARγ antagonist at the same time as ATRA resulted in a partial abrogation on the ATRA-mediated block in axial elongation. Therefore, our current findings, along with those previously reported for zebrafish [18], support the view that the activation of RARγ by physiological levels of ATRA functions to block stem/progenitor cell differentiation in developing tissues.

In addition to promoting the formation of totipotent 2CLCs in mouse ES cultures [30], RARγ ligation was shown repeatedly to have a positive effect on the establishment and/or maintenance of naïve-state pluripotency during the generation of induced pluripotent cells (iPSCs). Transgene expression of the orphan nuclear receptor, liver receptor homolog 1, reprogrammed Oct4-GFP epiblast stem cells into iPSCs and, post recovery from transgene expression, the addition of 0.1nM ATRA, to activate RARγ, into ATRA-free medium enhanced cellular reprogramming, whereas RARγ antagonism had a deleterious effect; further, this reprogramming enhancement required the presence of ATRA and was dependent on the presence of liganded RARγ [36]. For mouse embryonic fibroblasts (MEFs), adding transgene expression of RARγ and liver receptor homolog 1 to enhanced expression of Oct4, Sox2, c-Myc, and Klf4 promoted MEF reprogramming to iPSCs [37]. RARγ ligation had a positive effect of the generation of iPSCs derived from human dermal fibroblasts by transgene expression of Oct4, Sox2, Klf4, L-Myc, and p53, through the additional use of the RARγ agonist CD437 and the liver receptor homolog 1 agonist RJW101, along with inhibitors of glycogen synthase kinase-3 and mitogen-activated protein kinase kinase 1-2 [38]. These findings suggest that RARγ activation promotes the generation and/or proliferation of pluripotent stem cells, as well as their maintenance in an undifferentiated state.

It is possible, however, that the regulatory role of RARγ activity extends to stem/progenitor cell populations more widely than in embryonic development and pluripotency. In studies by Shimono and co-workers [39], the RARγ agonist NRX204647, and ATRA at concentrations of 3nM to 30nM, blocked ectopic bone formation in a transgenic model of fibrodysplasia ossificans progressiva. Bone morphogenetic proteins (BMPs) drive mesenchymal stem cell (MSC) differentiation towards chondrogenesis and osteogenesis in the developing limb [40] as well as in fracture repair [41] and *in vitro* treatment of mouse MSCs with the RARγ agonist rendered these cells unresponsive to BMP-2. The levels of Smad proteins were decreased within the RARγ agonist-treated MSCs [39]. Moreover, liganded RARγ interferes directly with Smad signaling as reported from transfection studies of lung

 doi:10.20944/preprints202603.2526.v1

fibroblast and HepG2 liver cells that made use of a Smad3 reporter, overexpression of individual RARs, and selective agonists and antagonists [42,43]. From these studies, RARγ bound to Smad3 and whereas liganded RARα and RARγ both applied a break to cell responsiveness to transforming growth factor (TGF)β, and non-liganded RARα and RARγ enhanced their responsiveness, inactive RARγ was more potent than RARα in modulating such TGFβ-dependent Smad3-mediated signaling. From the above, it is known that RARγ plays a non-canonical role as a co-factor to Smads in the regulation of TGFβ signaling.

Regarding the generation of iPSCs from epiblast stem cells, liganded RARγ had exerted a negative effect on Wnt signaling [36] and the enhancement of reprogramming of human dermal fibroblasts by liganded RARγ was attributed to a positive influence on TGFβ signaling [38]. Appropriate Wnt/β catenin signaling is essential in embryo axis formation and tissue organogenesis [43] and multiple Wnts and their receptors are regulated by RARs [44,45]. TGFβ signaling family members direct early stem/progenitor cell-fate decisions as master regulators of organogenesis [46]. RARγ is expressed predominantly in the cytoplasm of cholangiocarcinoma cells and colorectal cancer cells and RARγ activation of the Akt/NF-kB pathway and Wnt/β-catenin signaling has been reported for cholangiocarcinoma [47] and activation of Wnt/β-catenin signaling for colorectal cancer cells [48]. Hence, in our studies, agonizing RARγ may have interfered with Wnt/β catenin and/or TGFβ signaling to block gastruloid development. However, any RARγ-mediated events that block gastruloid development may be more complex than direct effects on Wnt/β-catenin or TGFβ signaling because RARγ activity regulates the expression of hundreds of genes, either directly or indirectly, as was seen from studies of ATRA-induced differentiation of F9 mouse ES cells [48]. RARγ also was shown to either positively or negatively regulate the expression of multiple genes in studies of RARγ knockouts in human squamous cell carcinoma cells. The genes regulated are known to play key roles in development [49]. For knockout squamous cell carcinoma cells without added RAR ligand, transcripts for NOTCH1, NOTCH3, and the NOTCH ligands, JAG2 and DLL1 were reduced [50]. Expression of these genes is associated with stratified squamous cell differentiation. Loss of RARγ binding also reduced expression of a broad group of genes that regulate cell identity and extracellular matrix communication, whilst genes that showed higher expression in the knockout cells and, therefore, were repressed by RARγ, included *RARG*, *PPARG*, and *RXRA*. RARγ control of the expression of *RXRA* is important because RXRα has multiple dimerization partners. Even so, it is important to bear in mind that these findings are for squamous cell carcinoma cells and RARγ acts within cells in a manner that is context dependent.

How agonism of RARγ activity blocks gastruloid development is yet unclear because there is uncertainty regarding whether the outcome from treating gastruloids with the RARγ agonist relates to an action against ES cells and/or committed progenitor cells. Moreover, RARγ may play many different regulatory roles. The multifaceted roles of RARγ include the direct regulation of gene expression and roles as a co-factor to other transcription factors and within the cytoplasm to modulate intracellular signaling. These varied roles may ensure tight regulation of the behavior of stem/progenitors whereby RARγ integrates multiple processes and findings to date highlight RARγ modulation of the responsiveness of stem/progenitor cells to extracellular signals that play a key role in governing changes to their behavior. Nonetheless, this study has further highlighted that the activation level of RARγ plays a key role in determining whether stem cells progress to enable tissue formation and development.

4. Materials and Methods

4.1. Single Cell RNA-Seq Analysis

Single cell RNA-seq data for gastruloids across 4 time points produced by REF was downloaded from the Gene Expression Omnibus (GEO, NCBI), accession number: GSE158999. The downloaded data was already aligned, clustered and the cluster cell types identified as detailed in Rossi et al., [33]. The data was loaded into R v4.2.2 and analysed using the Seurat package v4 [51]. Volcano plots

 doi:10.20944/preprints202603.2526.v1

showing gene expression for targets in different clusters were produced using the vlnplot function in Seurat.

For pairwise comparison of gene expression visualised as a Pearson correlation heatmap the data was converted to metacell data. This helps to overcome the sparsity of the single cell data and enables correlations to be calculated. Metacells were constructed using the hdWCGNA package [52] and expression was normalised using the NormalizeMetacells function. Scatter plots for pairwise gene comparison with calculated Pearson correlation values were then plotted using the ggplot2 package.

4.2. Retinoids

The binding affinities and specificities of the selective and stable RARα and RARγ agonists and antagonists have been described previously [32]. Both agonists do not transactivate retinoid X receptors. RARβ shows some response to the RARγ agonist, but this only occurs at high, non-physiological doses, i.e., greater than 100nM and was not a confounding issue regarding the doses used in experiments. The retinoids were synthesized at the Shanghai Institute of Materia Medica. They were dissolved in dimethylsulphoxide (DMSO) at a concentration of 10 mM (stored at -20^0 C), and this stock was diluted using culture medium to the required concentration. ATRA, which also was dissolved in DMSO, was purchased from Sigma-Aldrich (R2625, St Louis, MO, USA).

4.3. Routine ES cell culture

Wild-type E14-Tg2A (Hooper et al., 1987) mouse ES cells were seeded at a density of 1.2 x 10^4 cells/cm^2 on 0.1% (v/v) gelatin-coated flasks in GMEM (Gibco) supplemented with 15% foetal bovine serum (FBS; Gibco Cat. No. 10270-106), non-essential amino acids (Gibco; 11140035), sodium pyruvate (Gibco; 11360039), Glutamax™ (Gibco; 35050038), 2-mercaptoethanol (Gibco; 31350010), and LIF (QKine; QK018); hereon referred to as ESL medium. Cells were cultured in a humidified incubator maintained at 37°C with 5% CO2, and passaged every other day, with full medium changes on non-passage days. Cells were tested monthly and certified negative for mycoplasma.

4.4. Generation of gastruloids and treatments with ATRA and synthetic retinoids

Gastruloids were generated as previously described [21]. Briefly, 350 viable ES cells/well were plated in low-adherence U bottomed 96-well plates using a multichannel pipette in 40µl N2B27 medium and left to aggregate for 48 hours at 37^{o}C with 5% CO_2, after which 150µl of N2B27 medium supplemented with 3µM CHIR was added with 10nM ATRA or with specific 10nM RAR agonists/antagonists or with/without the DMSO carrier control, where the DMSO was diluted to the highest concentration of ATRA or added synthetic retinoid of combinations. At 72 hours and 96 hours after aggregation, 150µl medium was removed from each well using a multichannel pipette and replaced with fresh N2B27 medium minus the additional ATRA or retinoids. Samples were imaged by brightfield microscopy (see below) and fixed at 120 hours.

4.4. Immunostaining

Cells grown as gastruloids were fixed in 4% (v/v) formaldehyde in phosphate buffered saline (PBS) for half an hour at room temperature, after which they were briefly rinsed with PBS supplemented with 10% FBS and 0.2% Tween20 (PBSFT), followed by multiple hour-long incubations in PBSFT. Samples were then incubated with primary antibodies: goat anti-TBXT (PA5-46984; ThermoFisher; 1:50) and rabbit anti-Sox2 (AB5603; Abcam; 1:200) (diluted in PBSFT) and incubated overnight at 4 °C. Primary antibodies were then removed, samples rinsed briefly three times in PBSFT, followed by multiple hour-long washes in PBSFT. Samples were incubated with secondary antibodies: donkey anti-goat Alexa Fluor 568 (A-11057; Invitrogen; 1:500) and donkey anti-rabbit Alexa Fluor 488 (A-21206; Invitrogen; 1:500) (diluted in PBSFT) and incubated overnight at 4 °C. DAPI was also included (1:1000) as a counterstain to mark nuclei. Following multiple rinses in PBS

 doi:10.20944/preprints202603.2526.v1

supplemented with 0.2% FBS and Tween20, gastruloids were mounted between glass slides (No. 1 thickness) in Rapiclear, and adhesive spacers were used to ensure they were not compressed. Samples were stored at 4 °C until required.

4.5. Microscopy and Image Analysis

Live gastruloid brightfield images were acquired using a Nikon Ti-E inverted widefield microscope in a humidified incubator (37 °C, 5% CO_2). Imaging was performed using a 20x long working distance phase-contrast objective (NA 0.35, Ph1) with correction collar set to image through plastic. Transmitted light images were captured using a digital camera with an exposure time of 43ms and recorded using Nikon- Elements software. For immunofluorescence analysis, fixed, stained and mounted gastruloids were imaged using an Andor Dragonfly spinning disk confocal system mounted on a Leica DMi8 inverted microscope, using a 25x water-immersion objective (0.95 NA). Fluorophores were excited sequentially using 405 nm, 488 nm, and 561 nm laser diodes respectively, and emitted light reflected through 450/50 for DAPI, 525/20 for Alexa Fluor 488, and 620/60 for Alexa Fluor 568 bandpass filters, respectively. Emitted light was captured using an iXon Ultra 888 EM-CCD camera, with 1x1 binning, and recorded using Fusion software. Z-stacks were captured at Nyquist sampling intervals. Microscopy images were processed in the ImageJ package Fiji. The length and elongation index (length/largest circle that fits within the gastruloid area) were measured as previously described [21,53].

4.6. Statistical Analysis

At least 3 independent experiments (biological repeats) were performed, each with multiple technical repeats (minimum 3 repeats) for all analyses. Data were pooled and normality testing was assessed using the Shapiro–Wilk test, and significance determined using a non-parametric Kruskal-Wallis rank sum test using the Benjamini-Hochberg Procedure to correct for multiple comparisons. All data analysis, statistical tests, and graphing were performed in RStudio (2023.12.1+402). Data have been shown as histograms and box and whisker plots with overlaid data points. P values <0.05 were considered significant.

Author Contributions: Conceptualization: JTO, GB, WEBJ; Methodology: JTO, BEW, CMcQ; Validation: JTO, BEW, GB, CMcQ, WEBJ; Formal Analysis: JTO, B-EW GB, WEBJ; Investigation: JTO, BEW; Resources: CMcQ, GB, WEBJ; Data Curation, JTO, BEW, GB, WEBJ; Writing – Original Draft Preparation: JTO, BEW, GB, WEBJ; Writing – Review & Editing: CMcQ, GB, WEBJ; Supervision: GB, WEBJ; Funding Acquisition, GB, WEBJ. All authors have approved the submitted version and agree to be personally accountable for their contributions.

Funding: WEBJ was funded in this work by the University of Chester 2022/23 QR Fund grant no. 10M00037. GB was funded by UK Research and Innovation (UKRI) under the UK government's Horizon Europe funding guarantee EP/Y030818/1 and is an associate partner to the EU-funded doctoral network eRaDicate.

Institutional Review Board Statement: Not applicable as the study used established mouse cell lines only and did not require ethical approval.

Data Availability Statement: The original contributions presented in this study are included in the article/supplementary material. Further inquiries can be directed to the corresponding author(s).

Acknowledgments: We are grateful to Dr David Turner, University of Liverpool for the provision of E12Tg2a cells and for advice and input in the experimentation and confocal microscopy.

Conflicts of Interest: The authors declare no conflicts of interest.

References

1. Duester G. Retinoic acid synthesis and signaling during early organogenesis. *Cell*, **2008**, *134*, 921-931.
2. Rhinn, M; Dollé, P. Retinoic acid signalling during development. D*evelopment*, **2012**,*139*, 843-58.

 doi:10.20944/preprints202603.2526.v1

3. Berenbguer, M; Duester, G. Retinoic acid, RARs and early development. *J Mol Endocrinol*., **2022**, *69*, 59–67.
4. Rossant, J.; Zirngibl, R.; Cado, D.; Shago, M.; Giguère, V. Expression of a retinoic acid response element-hsplacZ transgene defines specific domains of transcriptional activity during mouse embryogenesis. *Genes Dev*., **1991**, *5*, 1333–1344.
5. Duester, G. Early retinoic acid signaling organizes the body axis and defines domains for the forelimb and eye. *Curr Top Dev Biol*., **2025,** *161*, 1-32.
6. Sandell, L.L.; Sanderson, B.W.; Moiseyev, G.; Johnson, T.; Mushegian, A.; Young, K.; Rey, J-P.; Ma, J-X.; Staehling-Hampton, K.; Trainor, P.A. RDH10 is essential for synthesis of embryonic retinoic acid and is required for limb, craniofacial, and organ development. *Genes Dev*., **2007**, *21*, 1113-1124.
7. Clagett-Dame, M.; Knutson, D. Vitamin A in reproduction and development. Nutrients, 2011, 3, 385-428.
8. Kam, R.K.; Shi, W.; Chan, S.O.; Chen, Y.; Xu, G.; Lau, C.B.; Fung, K.P.; Chan, W.Y.; Zhao, H. Dhrs3 protein attenuates retinoic acid signaling and is required for early embryonic patterning. *J Biol Chem*., **2013**, *288*, 31477-87.
9. Roeske TC, Scharff C, Olson CR, Nshdejan A, Mello CV. Long-distance retinoid signaling in the zebra finch brain. *PLoS One*., **2014**, *9*, e111722.
10. Hashimoto AS, Yu J, Williams C, Gaudenz K, Varshosaz P, Zhao R, Pilli N, Liu T, Russell J, Tooze RS, Twigg SRF, Banka S, Sweeney E, McGowan SJ, Knight SJL, Taylor JC, Froukh TJ, Palafoll MIV, Martínez-Gil N, Costa-Roger M, Villarreal-Molina MT, Lieberman Hernandez E, Abou Jamra R, Gattermann F, Koch-Hogrebe M, Wieczorek D, Trainor PA, Moise AR, Wilkie AOM, Kane MA. Identification and characterization of short-chain dehydrogenase/reductase 3 (DHRS3) deficiency, a retinoic acid embryopathy of humans. *Genet Med Open*., **2025**, *3*, 103427.
11. Uehara, M.; Yashiro, K.; Takaoka, K.; Yamamoto, M.; Hamada, H. Removal of maternal retinoic acid by embryonic CYP26 is required for correct Nodal expression during early embryonic patterning. *Genes Dev*., **2009**, *23*, 1689-98.
12. Fujii, H.; Sato, T.; Kaneko, S.; Gotoh, O.; Fujii-Kuriyama, Y.; Osawa, K.; Kato, S.; Hamada, H. Metabolic inactivation of retinoic acid by a novel P450 differentially expressed in developing mouse embryos. *EMBO J*., **1997**, *16*, 4163-73.
13. Sakai, Y.; Meno, C.; Fujii, H.; Nishino, J.; Shiratori, H.; Saijoh, Y.; Rossant, J.; Hamada, H. The retinoic acid-inactivating enzyme CYP26 is essential for establishing an uneven distribution of retinoic acid along the anterio-posterior axis within the mouse embryo. *Genes Dev*, **2001**, *15*, 213-25.
14. Ribes V, Fraulob V, Petkovich M, Dollé P. The oxidizing enzyme CYP26a1 tightly regulates the availability of retinoic acid in the gastrulating mouse embryo to ensure proper head development and vasculogenesis. *Dev Dyn*, **2007**, *236*, 644-53.
15. Shaker, M.R.; Lee, J.H.; Park, S.H.; Kim, J.Y.; Son, G.H.; Son, J.W.; Park, B.H.; Rhyu, I.J.; Kim, H.; Sun, W. Anteroposterior Wnt-RA gradient defines adhesion and migration properties of neural progenitors in developing spinal cord. *Stem Cell Reports*, **2020**, *15*, 898-911.
16. Yamanaka, Y.; Hamidi, S.; Yoshioka-Kobayashi, K.; Munira, S.; Sunadome, K.; Zhang, Y.; Kurokawa, Y.; Ericsson, R.; Mieda, A.; Thompson, J.L.; Kerwin, J.; Lisgo, S.; Yamamoto, T.; Moris, N.; Martinez-Arias, A.; Tsujimura, T.; Alev, C. Reconstituting human somitogenesis in vitro. *Nature*, **2023**, *614*, 509-520.
17. Chambon, P. A decade of molecular biology of retinoic acid receptors. *FASEB J*, **1996**, *10*, 940-54.
18. Wai, H.A.; Kawakami, K.; Wada, H.; Müller, F.; Vernallis, A.B.; Brown, G.; Johnson, W.E. The development and growth of tissues derived from cranial neural crest and primitive mesoderm is dependent on the ligation status of retinoic acid receptor gamma: evidence that retinoic acid receptor gamma functions to maintain stem/progenitor cells in the absence of retinoic acid. *Stem Cells Dev*., **2015,** *24*, 507-19.
19. Brown, G. Retinoic acid receptor regulation of decision-making for cell differentiation. *Front Cell Dev Biol*., **2023**, *11*, 1182204.
20. Ren, H.; Jia, X.; Yu, L. The building blocks of embryo models: embryonic and extraembryonic stem cells. *Cell Discov*., **2025**, *11*, 40.
21. Turner, D.A.; Girgin, M.; Alonso-Crisostomo, L.; Trivedi, V.; Baillie-Johnson, P.; Glodowski, C.R.; Hayward, P.C.; Collignon, J.; Gustavsen, C.; Serup, P.; Steventon, B.; Lutolf, M.P.; Arias, A.M. Anteroposterior polarity

 doi:10.20944/preprints202603.2526.v1

and elongation in the absence of extra-embryonic tissues and of spatially localised signalling in gastruloids: mammalian embryonic organoids. *Development*, **2017**, **144,** 3894-3906.

22. Siggia, E.D.; Warmflash A. Modeling mammalian gastrulation with embryonic stem cells. *Curr Top Dev Biol*, **2018,** *129*, 1-23.
23. Suppinger, S.; Zinner, M.; Aizarani, N.; Lukonin, I.; Ortiz, R.; Azzi, C.; Stadler, M.B.; Vianello, S.; Palla, G.; Kohler, H.; Mayran, A.; Lutolf, M.P.; Liberali P. Multimodal characterization of murine gastruloid development. *Cell Stem Cell*, **2023**, *30*, 867-884.
24. Mantziou, V.; Baillie-Benson, P.; Jaklin, M.; Kustermann, S.; Arias, A.M.; Moris N. In vitro teratogenicity testing using a 3D, embryo-like gastruloid system. *Reprod Toxicol.*, **2021**, *105*, 72-90.
25. Hamazaki, N.; Yang, W.; Kubo, C.A.; Qiu, C.; Martin, B.K.; Garge, R.K.; Regalado, S.G.; Nichols, E.K.; Pendyala, S.; Bradley, N.; Fowler, D.M.; Lee, C.; Daza, R.M.; Srivatsan, S.; Shendure J. Retinoic acid induces human gastruloids with posterior embryo-like structures. *Nat Cell Biol.*, **2024**, *26*, 1790-1803.
26. De Leenheer, A.P.; Lambert, W.E.; Claeys I. All-trans-retinoic acid: measurement of reference values in human serum by high performance liquid chromatography. *J Lipid Res.*, **1982**, *23*, 1362–1367.
27. Eckhoff, C.; Nau, H. Identification and quantitation of all-trans- and 13-cis-retinoic acid and 13-cis-4-oxo-retinoic acid in human plasma. *J Lipid Res.*, **1990**, *31*, 1445–1454.
28. Brown, G. Deregulation of all-trans retinoic acid signaling and development in cancer. *Int. J. Mol. Sci.* **2023,** *24*, 12089.
29. Li, Y.; Mao, X.; Zhou, X.; Su, Y.; Zhou, X.; Shi, K.; Zhao, S. An optimized method for neuronal differentiation of embryonic stem cells in vitro. *Neurosci Methods*, **2020,** *15*, 330:108486.
30. Iturbide, A.; Ruiz Tejada Segura, M.L.; Noll, C.; Schorpp, K.; Rothenaigner, I.; Ruiz-Morales, E.R.; Lubatti, G.; Agami, A.; Hadian, K.; Scialdone, A.; Torres-Padilla, M.E. Retinoic acid signaling is critical during the totipotency window in early mammalian development. *Nat Struct Mol Biol.*, **2021**, *28*, 521-532.
31. Oeda, S.; Hayashi, Y.; Chan, T.; Takasato, M.; Aihara, Y.; Okabayashi, K.; Ohnuma, K.; Asashima, M. Induction of intermediate mesoderm by retinoic acid receptor signaling from differentiating mouse embryonic stem cells. *Int J Dev Biol.*, **2013**, *57*, 383-9.
32. Hughes, P.J.; Zhao, Y.; Chandraratna, R.A.; Brown, G. Retinoid-mediated stimulation of steroid sulfatase activity in myeloid leukemic cell lines requires RAR alpha and RXR and involves the phosphoinositide 3-kinase and ERK-MAP kinase pathways. *J of Cell Biochem.*, **2006**, 97, 327-350.
33. Rossi, G.; Broguiere, N.; Miyamoto, M.; Boni, A.; Guiet, R.; Girgin, M.; Kelly, R.G.; Kwon, C.; Lutolf, M.P. Capturing cardiogenesis in gastruloids. *Cell Stem Cell,* 2021, *28*, 230-240.
34. Braccioli, L.;,van den Brand, T.; Alonso Saiz, N.; Fountas, C.; Celie, P.H.N.; Kazokaitė-Adomaitienė, J.; de Wit E. Identifying cross-lineage dependencies of cell-type-specific regulators in mouse gastruloids. *Dev Cell*. **2025**, *60*, 2007-2022.
35. Fiuza, U.M.; Bonavia, S.; Pascual-Mas, P.; Torregrosa-Cortés, G.; Casaní-Galdón, P.; Robertson, G.; Dias, A.; Martinez Arias, A. Morphogenetic constraints in the development of gastruloids: Implications for mouse gastrulation. *Cells Dev.* **2025,** *183*, 204043.
36. Yang, J.; Wang, W.; Ooi, J.; Campos, L.S.; Lu, L.; Liu, P. Signalling Through Retinoic Acid Receptors is Required for reprogramming of both mouse embryonic fibroblast cells and epiblast stem cells to induced pluripotent stem cells. *Stem Cells.* **2015,** *33*, 1390-404.
37. Wang, W.; Yang, J.; Liu, H.; Lu, D.; Chen, X.; Zenonos, Z.; Campos, L.S.; Rad, R.; Guo, G.; Zhang, S.; Bradley, A.; Liu, P. Rapid and efficient reprogramming of somatic cells to induced pluripotent stem cells by retinoic acid receptor gamma and liver receptor homolog 1. *Proc Natl Acad Sci U S A.* **2011**, *108*, 18283-8.
38. Taei, A.; Kiani, T.; Taghizadeh, Z.; Moradi, S.; Samadian, A.; Mollamohammadi, S.; Sharifi-Zarchi, A.; Guenther, S.; Akhlaghpour, A.; Asgari Abibeiglou, B.; Najar-Asl, M.; Karamzadeh, R.; Khalooghi, K.; Braun, T.; Hassani, S.N.; Baharvand, H. Temporal activation of LRH-1 and RAR-γ in human pluripotent stem cells induces a functional naïve-like state. *EMBO Rep.*, **2020**, *21*, e47533.
39. Shimono, K.; Tung, W.E.; Macolino, C.; Chi, A.H.; Didizian, J.H.; Mundy, C.; Chandraratna, R.A.; Mishina, Y.; Enomoto-Iwamoto, M.; Pacifici, M.; Iwamoto, M. Potent inhibition of heterotopic ossification by nuclear retinoic acid receptor-γ agonists. *Nat Med.*, **2011**, *17*, 454-60.

 doi:10.20944/preprints202603.2526.v1

40. Beederman, M.; Lamplot, J.D.; Nan, G.; Wang, J.; Liu, X.; Yin, L.; Li, R.; Shui, W.; Zhang, H.; Kim, S.H.; Zhang, W.; Zhang, J.; Kong, Y.; Denduluri, S.; Rogers, M.R.; Pratt, A.; Haydon, R.C.; Luu, H.H.; Angeles, J.; Shi, L.L.; He, T.C. BMP signaling in mesenchymal stem cell differentiation and bone formation. *J Biomed Sci Eng.*, **2013**, *6*, 32-52.
41. Zhou, L.; Wang, J.; Mu, W. BMP-2 promotes fracture healing by facilitating osteoblast differentiation and bone defect osteogenesis. *Am J Transl Res*., **2023**, *15*, 6751-6759.
42. Pendaries, V.; Verrecchia, F.; Michel, S.; Mauviel, A. Retinoic acid receptors interfere with the TGF-beta/Smad signaling pathway in a ligand-specific manner. *Oncogene*, **2003**, *22*, 8212-20.
43. Brown G. The influences of RARγ on the behavior of normal and cancer stem cells. *Int J Mol Sci*., **2026,** *27*, 1291.
44. Qin, K.; Yu, M.; Fan, J.; Wang, H.; Zhao, P.; Zhao, G.; Zeng, W.; Chen, C.; Wang, Y.; Wang, A.; Schwartz, Z.; Hong, J.; Song, L.; Wagstaff, W.; Haydon, R.C.; Luu, H.H.; Ho,S.H.; Strelzow, J.; Reid, R.R.;He, T.C.; Shi, L.L. Canonical and noncanonical Wnt signaling: Multilayered mediators, signaling mechanisms and major signaling crosstalk. *Genes Dis.* **2023**, *11*, 103-134.
45. Osei-Sarfo, K.; Gudas, L.J. Retinoic acid suppresses the canonical Wnt signaling pathway in embryonic stem cells and activates the noncanonical Wnt signaling pathway. Stem Cells, **2014,** *32*, 2061–2071.
46. Mullen, A.C.; Wrana, J.L. TGF-β family signaling in embryonic and somatic stem-cell renewal and differentiation. *Cold Spring Harb Perspect Biol*., **2017**, *9*, a022186.
47. Huang, G.L.; Luo, Q.; Rui, G.; Zhang, W.; Zhang, Q.Y.; Chen, Q.X.; Shen, D.Y. Oncogenic activity of retinoic acid receptor γ is exhibited through activation of the Akt/NF-κB and Wnt/β-catenin pathways in cholangiocarcinoma. *Mol Cell Biol*., **2013**, *33*, 3416-25.
48. Huang, G.L.; Song, W.; Zhou, P.; Fu, Q.R.; Lin, C.L.; Chen, Q.X.; Shen, D.Y. Oncogenic retinoic acid receptor γ knockdown reverses multi-drug resistance of human colorectal cancer via Wnt/β-catenin pathway. *Cell Cycle*, **2017**, *16*, 685-692.
49. Mendoza-Parra, M.A.; Walia, M.; Sankar, M.; Gronemeyer, H. Dissecting the retinoid-induced differentiation of F9 embryonal stem cells by integrative genomics. *Mol Syst Biol*., **2011**, *11*, 538.
50. Hoxie, H.R.; Tang, X.H.; Gudas, L.J. Multiple modes of transcriptional regulation by the nuclear hormone receptor RARγ in human squamous cell carcinoma. *J Biol Chem*., **2026**, *302*, 110965.
51. Hao, Y.; Hao, S.; Andersen-Nissen, E.; Mauck, W.M. 3rd; Zheng, S.; Butler, A.; Lee, M.J.; Wilk, A.J.; Darby, C.; Zager, M.; Hoffman, P.; Stoeckius, M.; Papalexi, E.; Mimitou, E.P.; Jain, J.; Srivastava, A.; Stuart, T.; Fleming, L.M.; Yeung, B.; Rogers, A.J.; McElrath, J.M.; Blish, C.A.; Gottardo, R.; Smibert. P.; Satija R. Integrated analysis of multimodal single-cell data. *Cell*, **2021**, *184*, 3573–3587.
52. Morabito, S.; Reese, F.; Rahimzadeh, N.; Miyoshi, E.; Swarup, V. hdWGCNA identifies co-expression networks in high-dimensional transcriptomics data. *Cell Rep Methods*, **2023**, *3*, 100498.
53. Girgin, M. U., Broguiere, N., Mattolini, L., & Lutolf, M. P. Gastruloids generated without exogenous Wnt activation develop anterior neural tissues. 2021, *Stem Cell Reports*, **2021**, *16*, 1143–1155.